CONF-950828--6

RHEOLOGICAL PROPERTIES OF THE PRODUCT SLURRY OF THE NITRATE TO AMMONIA AND CERAMIC (NAC) PROCESS

I. Muguercia, G. Yang, and M. A. Ebadian*
Department of Mechanical Engineering
Florida International University
Miami, FL 33199

D. D. Lee, A. J. Mattus, and R. D. Hunt
Chemical Technology Division
Oak Ridge National Laboratory
Oak Ridge, TN 37831

MASTER

DISTRIBUTION OF THIS DOCUMENT IS UNLIMITED

DLC

---

*ASME Fellow, The author to whom all correspondence should be addressed.

DISCLAIMER

ABSTRACT

The Nitrate to Ammonia and Ceramic (NAC) process is an innovative technology for immobilizing the liquid from Low Level radioactive Waste (LLW). An experimental study was conducted to measure the rheological properties of the pipe flow of the NAC product slurry. Test results indicate that the NAC product slurry has a profound rheological behavior. At low solids concentration, the slurry exhibits a typical dilatant fluid (or shear thickening) behavior. At high solids concentration, the slurry changes to a pseudo-plastic (or shear thinning) fluid. The transition from dilatant fluid to pseudo-plastic fluid will occur at between 25% to 30% solids concentration in temperature ranges of 50 - 80°C. Correlation equations are developed based on the test data.

NOMENCLATURE

d	pipe diameter, m
f	friction coefficient
K	fluid consistency, $N*sec^{3-n}m^{-2}$
L	pipe length, m
Re_g	general Reynolds number
u_m	slurry mean velocity, $m\ sec^{-1}$
V	volume flow rate, $m^3\ sec^{-1}$

Greek Symbols

Δp	pressure drop along the test section
γ	shear rate, sec^{-1}
μ_e	effective viscosity, $N\ sec^{2-n}$
ρ	slurry density, $kg\ m^{-3}$
τ	shear stress, $N\ m^{-2}$

Superscripts

n	flow index

I. INTRODUCTION

Over the past 50 years, millions of tons of low-level radioactive waste (LLW) have been generated at various U.S. weapons facilities. This LLW is stored mainly at five U.S. Department of Energy sites, Fernald, Hanford, Oak Ridge, Richland and Savannah River. More than three hundred underground storage tanks have been used to process and store LLW. Radioactive waste in the liquid state poses a great threat due to the potential for seepage into groundwater supplies. Therefore, it must be immobilized before final disposal. Preliminary studies have indicated that more than 80% of the chemical concentration in this LLW is composed of sodium nitrate with a radiation level of 0.1 to 1.2 R/h. The characteristics of this sodium nitrate–based waste, in addition to the levels of radioactivity, are as follows: pH, either <1 or >12, with a total salt content of $>5M$, and a sodium content of $>1.5M$. Currently, the most common immobilization method for the LLW is the use of cement-based grout. However, this method will increase the volume of the waste, does not effectively retain certain contaminants, and has questionable long term stability. Other alternative long term disposal methods, such as polyethylene and biodenitrification, are still in their early development stage.

Recently, a new immobilization technique for LLW, the Nitrate to Ammonia and Ceramic (NAC) process, has been developed (Mattus et al. 1993 and Mattus and Lee 1993). Instead of mixing the liquid waste directly with the cement to make concrete blocks, the NAC process eliminates the nitrate from the LLW by converting it to ammonia gas. Aluminum particles are used as a reductant to complete this conversion. The final product of the NAC process is gibbsite, which can be further sintered to a ceramic waste form. Radioactive species, such as plutonium and strontium, will enter the solid ceramic phase during the reduction process. The alumina-based ceramic will be further calcined pressed, and sintered to generate the solid waste form. Preliminary tests have indicated that the NAC process not only produces environmentally acceptable waste, but can also reduce the volume of the final waste by up to 70%, as compared with the cement-based grout method. This volume reduction represents a significant reduction in cost for final land disposal.

The NAC process is an exothermic process, which generates large amounts of heat during the chemical reaction. In order to maintain a desired operating temperature of between 50° to 85°C inside the NAC reactor, a cooling system is required. To design a cooling system and the NAC reactor, one needs to know the rheological behaviors of the product slurry. Past experience has shown that the product slurry of the NAC process behaves as a non-Newtonian fluid, and that the use of correlation equations from Newtonian fluids for design application could result in considerable error. Unfortunately, this information is not available in the open literature. Therefore, the objective of this study is to experimentally determine the rheological behavior of the final product slurry. In this paper, a description of the test facility is given first, and an error analysis of the test is then discussed. Finally, the experimental results of the rheological behavior of the product slurry are presented.

II. THE TEST APPARATUS

A test apparatus has been designed and constructed to measure the rheological properties and the friction coefficient of the pipe flow. Figure 1 illustrates the test facility, which consists of the NAC process reactor, the test loop, and the associated instrumentation. The NAC reactor is a 6 liter chemical reactor (model BioFlo IIC manufactured by New Brunswick Scientific), which automatically controls the slurry temperature. Non-radioactive gibbsite slurry, chemically and rheologically similar to the final product of the NAC process, was used to simulate the actual product slurry. The chemical compositions and the particle size distributions of the dried powder from the slurry are listed in Tables I and II, respectively. The gibbsite slurry is pumped from the reactor to a test loop and then discharged back to the reactor. The test loop is constructed of an 0.86" ID stainless steel pipe. The test loop has two sections: the test section and the temperature control section. The 8-ft-long test section is used to measure the pressure drop of the slurry pipe flow. The test section is insulated with fiberglass packing to maintain a constant temperature during the test. The 8-ft-long temperature control section is a double-pipe heat exchanger, that is used to provide additional temperature control for the slurry inside the reactor.

Table I Composition of the Dried Powder of the Slurry

Composition	Wt. %
H_2O	65.1
Sodium nitrate	34.4
Soluble sodium nitrate	0.05
SiO_2	0.03
Fe_2O_3	0.008
V_2O_5	0.002
Cu	0.001
Mn	0.0015

Table II Size Distributions of the Dried Powder of the slurry

Larger than 15 μm	10%
Between 7 and 15 μm	40%
Between 3 and 7 μm	40%
Smaller than 3 μm	10%

Two pressure transducers were connected to the inlet and outlet of this section. The uncertainty of the pressure measurement was ±0.5%. An FE-125 magnetic flowmeter was used to measure the slurry flow rate through the pipe. The uncertainty of the flow measurement is ±2 %. Two thermocouples were used to measure the slurry temperatures at both the inlet and outlet of this section. All thermocouples were connected to a Hewlett-Packard data acquisition system, and the temperatures were automatically recorded by a computer. The difference in the reading of all thermocouples was less than ±0.2 °C. The overall uncertainty of the temperature measurement was ±0.3 °C.

III. Data Reduction Methodology

During the test, the slurry flow rate, the temperature, and the pressure difference were continuously recorded. For the pipeline viscometer, the shear rate, shear stress, and the effective viscosity can be calculated based on this measured information (Irvine and Karni, 1987, and Wasp et. al. 1977).

The shear rate is determined by:

$$\gamma = 32\ V/d^3\ , \tag{1}$$

where V and d are the slurry volume flowrate and the pipe diameter, respectively. The shear stress can be found by:

$$\tau = d\ \Delta p/(4L)\ , \tag{2}$$

where L is the distance between the two pressure transducers, and Δp is the corresponding pressure drop. The effective viscosity can then be calculated by:

$$\mu_e = \tau\ \gamma^{-1} = K\ \gamma^{n-1}\ , \tag{3}$$

where the n and K are the flow index and fluid consistency, respectively. The Reynolds number is defined by:

$$Re_g = (\rho\, u_m^{2-n}\, d^n)/K\,, \tag{4}$$

where ρ and u_m are the density and the mean flow velocity of the slurry, respectively. Through the uncertainty analysis (Figliola and Beasley, 1991), the uncertainties of major parameters are listed in Table III.

Table III The Uncertainties of the Major Results

PARAMETERS	%
Shear rate	2.6
Shear stress	1.5
Effective viscosity	3.0
Reynolds number	3.5

IV Rheological Properties of the Product Slurry

Six solid concentration slurries, 17%, 20%, 23%, 30%, 33%, and 40% wt. of gibbsite by weight, have been tested. To ensure the repeatability of the test results during the test, the slurry was disposed of after finishing the test for certain solids concentrations. The repeated test for this solids concentration slurry was conducted using the separately mixed slurry. During the test, the slurry was kept at three constant temperatures, 50°C, 65°C, and 80°C, through a heater inside the reactor. In each case, the slurry flow rate was varied between 5 *l*/min to 37 *l*/min. The test conditions are listed in Table IV.

Table IV Test Conditions of the Pressure Measurement

Case	Gibbsite concentration wt. %	Slurry temperature °C	Slurry flow rate liters/min
1	17	50	5 - 37
2	17	80	5 - 37
3	20	50	5 - 37
4	20	65	5 - 37
5	20	80	5 - 37
6	23	50	5 - 37
7	23	65	5 - 37
8	23	80	5 - 37
9	30	50	5 - 37
10	30	65	5 - 37
11	30	80	5 - 37
12	33	50	5 - 37
13	33	65	5 - 37
14	33	80	5 - 37
15	40	50	5 - 37
16	40	65	5 - 37
17	40	80	5 - 37

The first step of the test was to determine whether the fluid's rheological property was time-independent fluid. For this test, the slurry flow was to be increased from the minimum value to the maximum value, and then reduced to the minimum value. The shear-stress/shear-rate relation indicated that the rheological property of the slurry was time-independent.

Figure 2 shows the effective viscosity changes with the slurry solids concentration at different shear rates. The figure indicates that at a high solids concentration (40% solids concentration, at 65°C and 80°C), the slurry exhibits a pseudo-plastic behavior—that is, the effective viscosity decreased as the shear rate increased. At low concentration (20% solids concentration, at 50°C and 80°C), the slurry exhibited a dilatant behavior, or the effective viscosity increased as the shear rate increased. In both cases, the rheological behavior of the slurry was not very sensitive to the temperature change. The rheological behavior of the 30% concentration slurry lies somewhere in between. The transition from dilatant flow to pseudo-plastic flow will be occur between the 25% to 30% concentration. The change in the rheological behavior of the slurry is due to the change in the water-bonding structures at different solids concentration. The physical appearance of the 20% slurry was a milk-like solution, while the 40% slurry was similar in appearance to yogurt or white paint. In the liquid/solid suspension fluid (slurry), the continuous liquid is called the dispersing phase, and the discontinuous particles are known as the dispersed phase. The rheological behavior of the slurry will depend on the rheological behavior of the dispersing phase and the size, shape, stiffness, concentration and degree of dispersion of the solid particles. When the particles tend to agglomerate together at rest, the slurry may exhibit as pseudo-plastic fluid. If the agglomeration of particles increases with shear rate, the slurry may exhibit dilatant behavior.

Figure 3 shows the shear stress and shear rate relation for the slurry with 17%, 20%, and 23% concentrations. The results indicate that the slurry exhibits a dilatant fluid behavior (or shear thickening)—that is, the shear stress increases rapidly as the shear rate increases. The shear-stress/shear-rate relation is independent of the slurry temperature and the solids concentration, and can be well correlated by the power law:

$$\tau = 1.267 \text{x}\ 10^{-4}\ \gamma^{1.74}\ , \qquad (5)$$

Figure 4 shows the slurry effective viscosity as a function of shear rate for the same case. The figure indicates that the slurry's effective viscosity increases from 6 cp ($N*s/m^2 *10^{-3}$) at γ=200 to 15 cp at $\gamma = 560$, and again, the change of the slurry temperature and solids concentration in this test region will not affect the slurry viscosity. For the power law fluid, the effective viscosity can be written as:

$$\mu_e = \tau \, \gamma^{-1} = 0.1267\gamma^{0.74} \; . \tag{6}$$

Figure 5 shows the friction coefficient changes with the general Reynolds number of the slurry. For the case in Fig. 3, the test range of the general Reynolds number in this study is approximately 12,000 to 15,000. Previous research has indicated that the transition occurs when Re_g exceeds approximately 2100 for a power law fluid in a circular tube, and the flow can be considered as turbulent when $Re_g > 3000$. Therefore, the test conducted for slurry below a 23% solids concentration was in the turbulent region. The correlation equation is adequate for the experimental data:

$$f = 2100/\, Re_g^{1.2} \; . \tag{7}$$

When the gibbsite concentration was higher than 40%, the rheological property of the slurry changed from a dilatant fluid (shear thickening) to a pseudo-plastic fluid (or shear thinning). Figure 6 shows the shear stress/shear rate relation for the 33% and 40% solids concentration slurry—that is, the shear stress increased as the shear rate increased. It can also be seen that the shear stress increased slightly as the slurry temperature increased. The test data can be correlated by:

$$\tau = 1.75\gamma^{0.27} \; . \tag{8}$$

Figure 7 shows the corresponding effective viscosity as a function of the shear rate change. The effective viscosity has a high value at a low shear rate, and gradually decreases to 20 cp when the shear stress increases to 500 s^{-1}. It can be seen that the effective viscosity of the high concentration slurry was much higher than that of the low solids concentration slurry. Although the effective viscosity is slightly affected by the slurry temperature, the test data can be well correlated by a regression equation with ± 15% deviations:

$$\mu_e = \tau \dot{\gamma}^{-1} = 1750\gamma^{-0.73} \quad . \qquad (9)$$

Figure 8 shows the friction coefficient changes with the general Reynolds number flow. Due to the high effective viscosity, the figure shows that the slurry flow was in the range where the general Reynolds number less than 600—that is, in the laminar flow region. The tested data can be correlated by:

$$f = 15.1/\, Re_g^{1.02} \quad . \qquad (10)$$

V. SUMMARY

Experimental study has been conducted to measure the rheological properties of the pipe flow for the NAC product slurry. The test results indicate that the NAC product slurry has a time independent non-Newtonian rheological behavior. At a low solids concentration, the slurry exhibits a dilatant fluid (or shear thickening) behavior, and at a high solids concentration, the slurry changes to pseudo-plastic (or shear thinning) fluid. Transition from the dilatant fluid to pseudo-plastic fluid will be occur between 25% to 30% solids concentration in the temperature ranges of 50 - 80 °C. The correlation equations have been developed from the test data. During operation of the NAC reactor, the solids concentration will be varied from 20% to 40%. Unfortunately, this study indicates that the slurry's rheological properties has a transition in this concentration range. To ensure safe operation and to obtain a desired final product, the design should consider the worst case. Therefore, the rheological values of 40% solid concentration slurry, which has the highest viscosity, is recommended for engineering design.

ACKNOWLEDGMENT

The results presented in this paper were obtained in the course of research sponsored by the Department of Energy's Office of Technology Development under Grant No. 19X-SN855C.

REFERENCES

Figliola R. S. and D. E. Beasley, *Theory and Design for Mechanical Measurements*, Chapter 5, John Wiley & Son, New York, 1991.

T. F. Irvine and J. Karni, "Non-Newtonian Fluid Flow and Heat Transfer," Chapter 20 of the *Handbook of Single Phase Convective Heat Transfer*, ed. by S. Kakac, R. K. Shah, and W. Aung, Wiley Interscience, New York, 1987.

Lima, G. G. C., R. F. Navarro, O. L. S. de Alsina, "Influence of the Concentration on the Power Law Index of Alumina Suspensions in High Viscosity Newtonian Fluids," Proceeding of 7th International Symposium on Transport Phenomena in Manufacturing Processes, Acapulco, Mexico, August, 1994.

A. J. Mattus, D. D. Lee, T. A. Dillon, E. L. Youngblood, T. Tiegs, and L. L. Farr, "A Low Temperature Process for the Denitration of the Hanford Single Shell Tank, Nitrate-Based Waste Utilizing the Nitrate to Ammonia and Ceramic (NAC) Process, Phase II Report," a report to the U. S. Department of Energy, DE-AC05-840R21400, Oak Ridge National Laboratory, 1993.

A. J. Mattus and D. D. Lee, "The Nitrate to Ammonia and Ceramic (NAC) Process-A Newly Developed Low Temperature Technology," Second International Mixed Waste Symposium, Aug. 17-20, 1993, Baltimore, Maryland, 1993.

E. J. Wasp, J. P. Kenny, and R. L. Gandhi, *Solid-Liquid Flow Slurry Pipeline Transportation*, Trans Tech Publications, Clausthal, Germany, 1977.

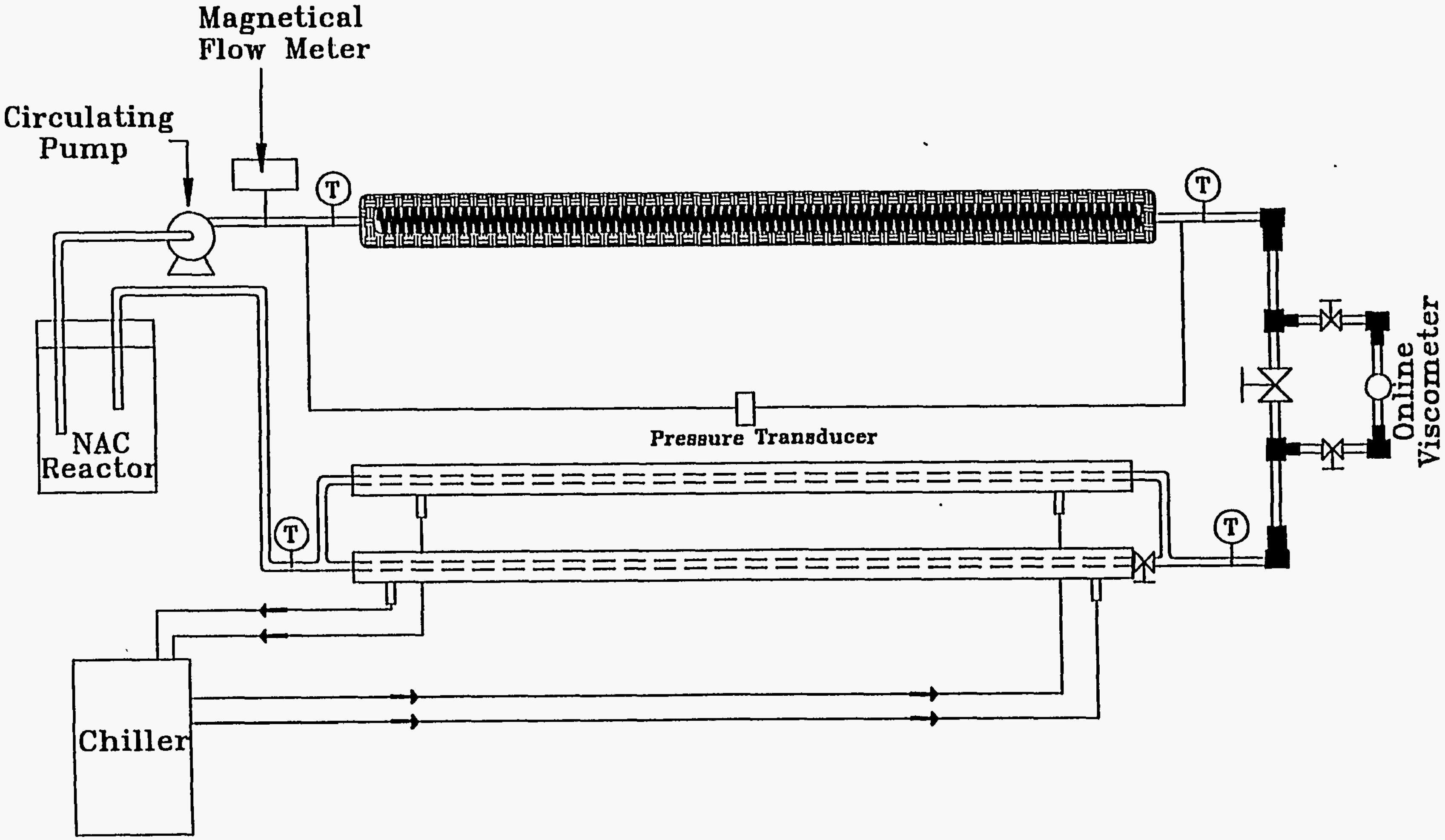

Fig. 1 Schematic of the test loop.

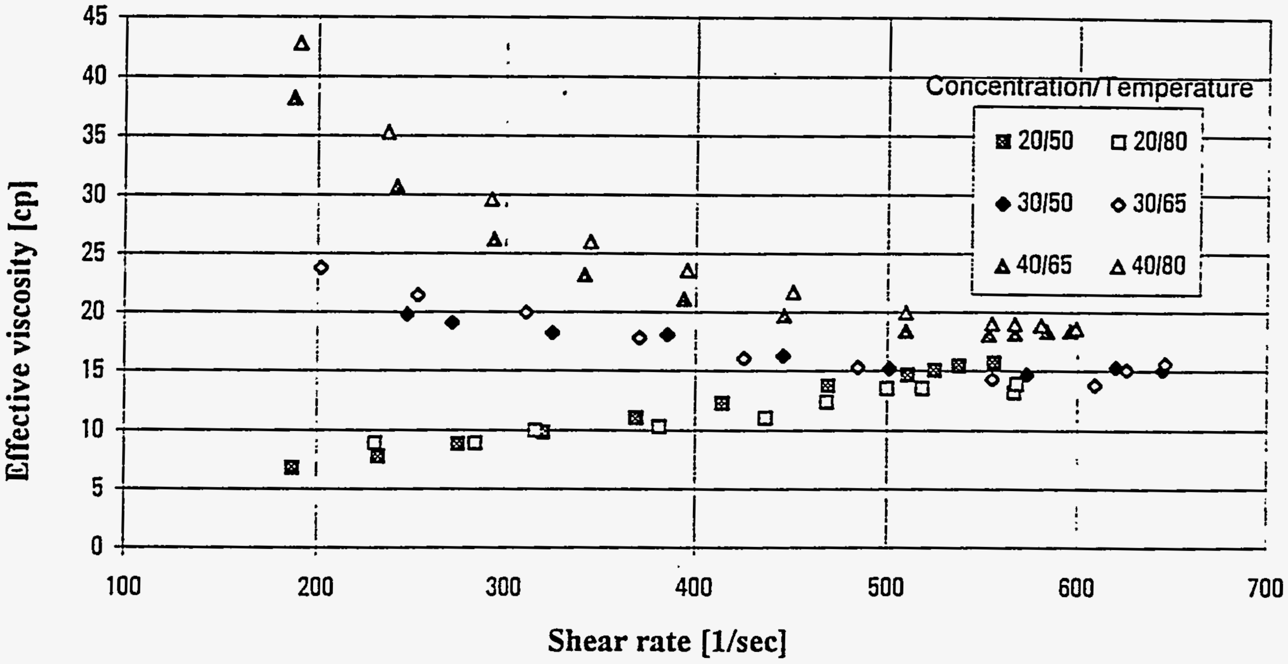

Fig. 2 Effective viscosity changes with the shear rate.

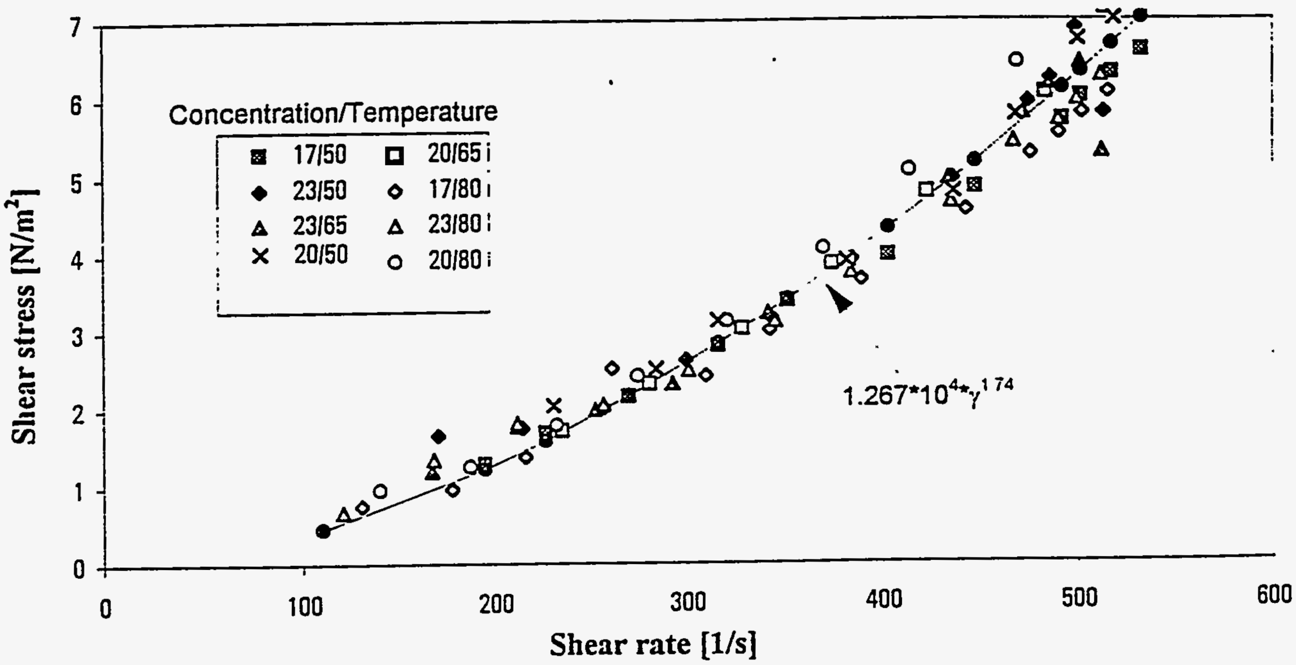

Fig. 3 Shear stress as a function of the shear rate for low solids concentration slurry.

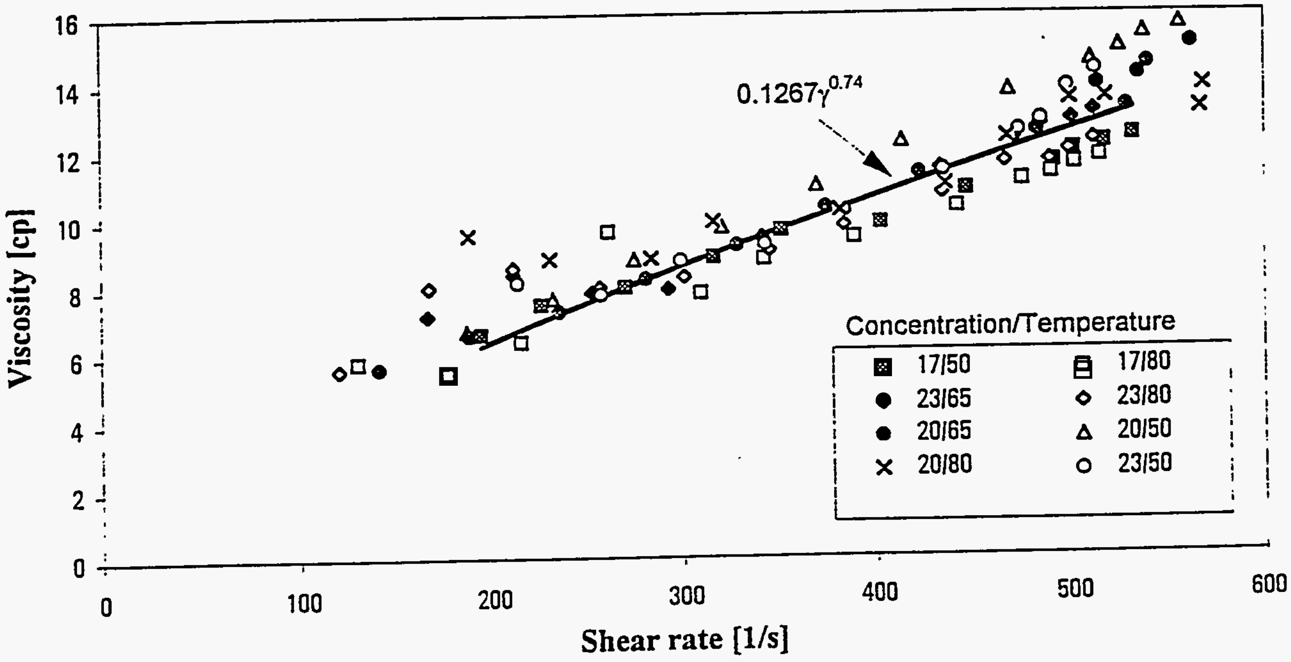

Fig. 4 Effective viscosity as a function of the shear rate for low solids concentration slurry.

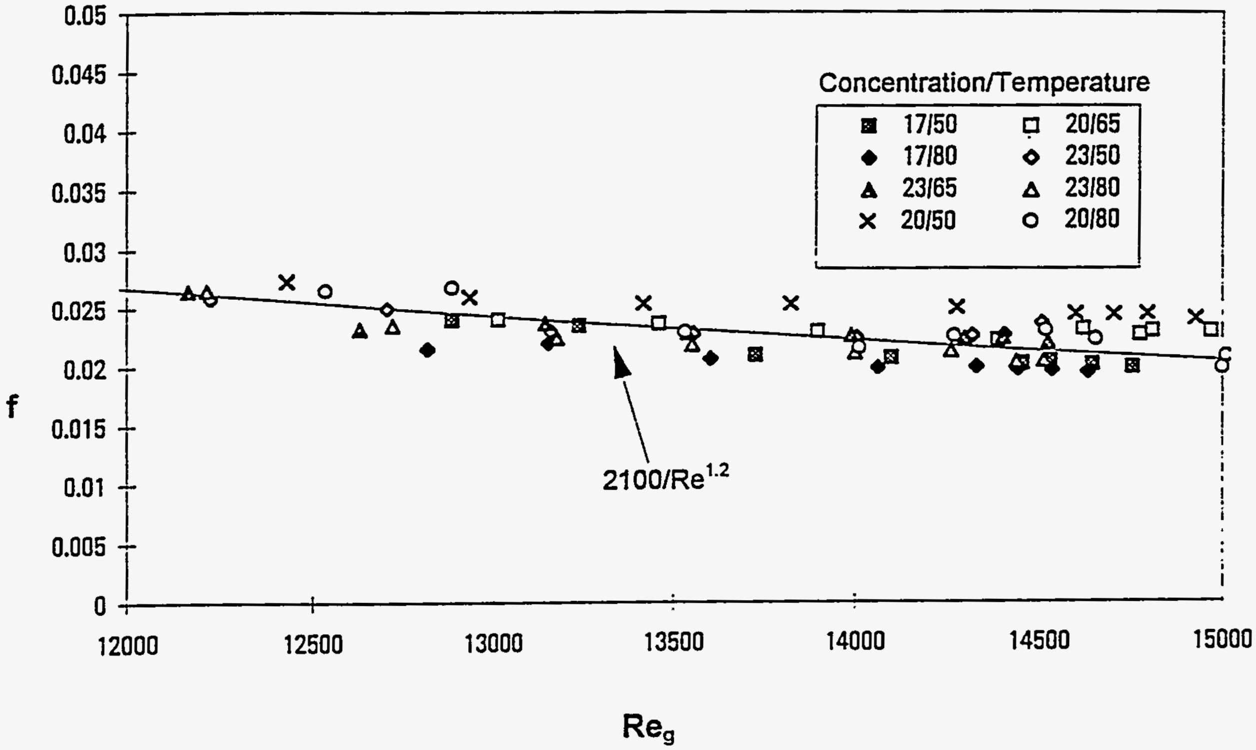

Fig. 5 Friction coefficient changes with the general Reynolds number.

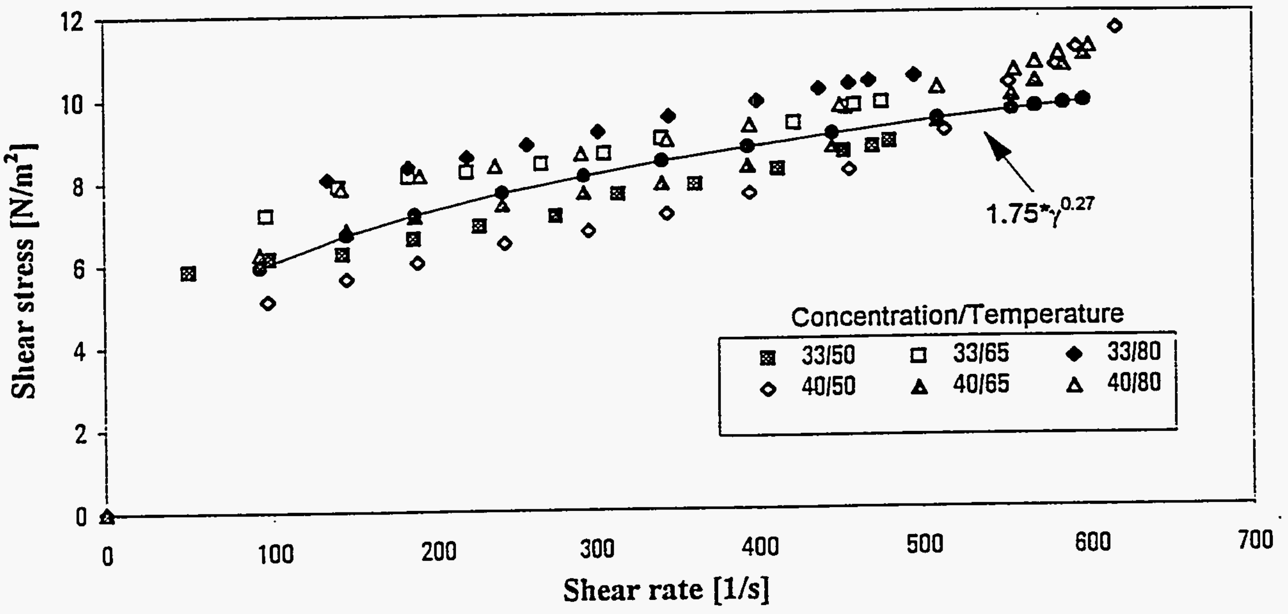

Fig. 6 Shear stress as a function of the shear rate for high solids concentration slurry.

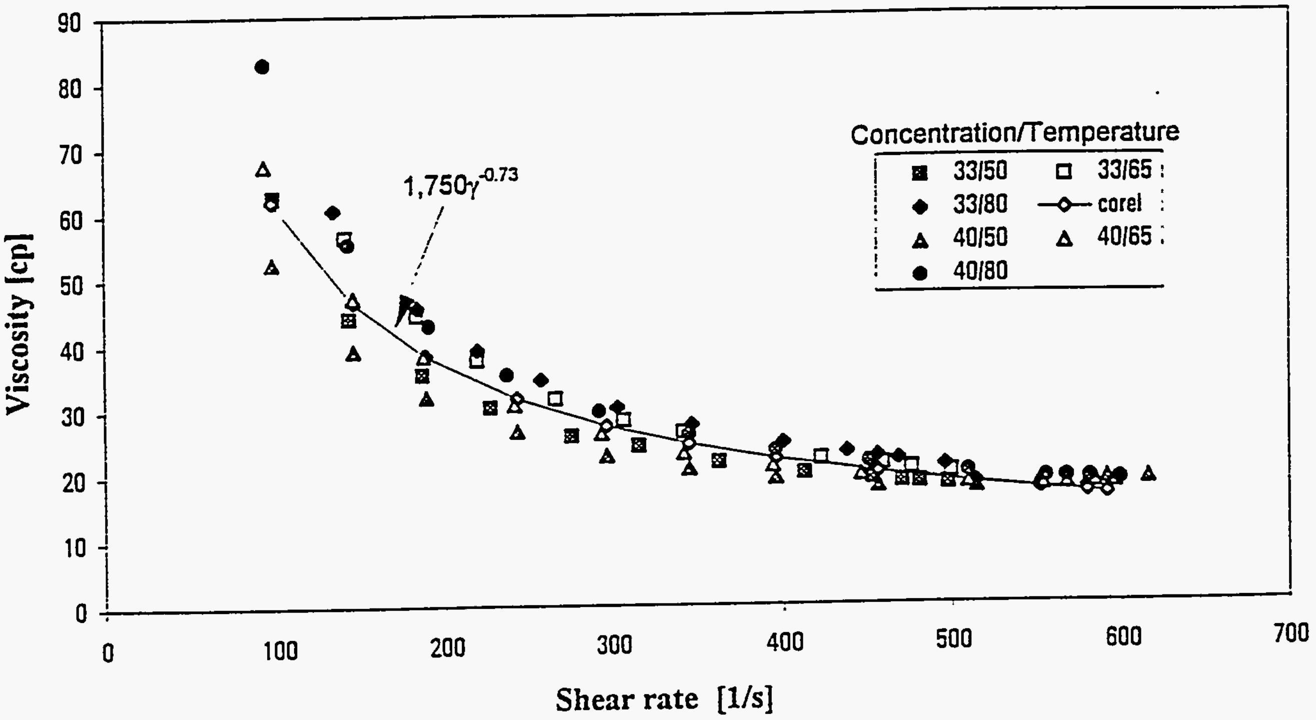

Fig. 7 Effective viscosity as a function of the shear rate for high solids concentration slurry.

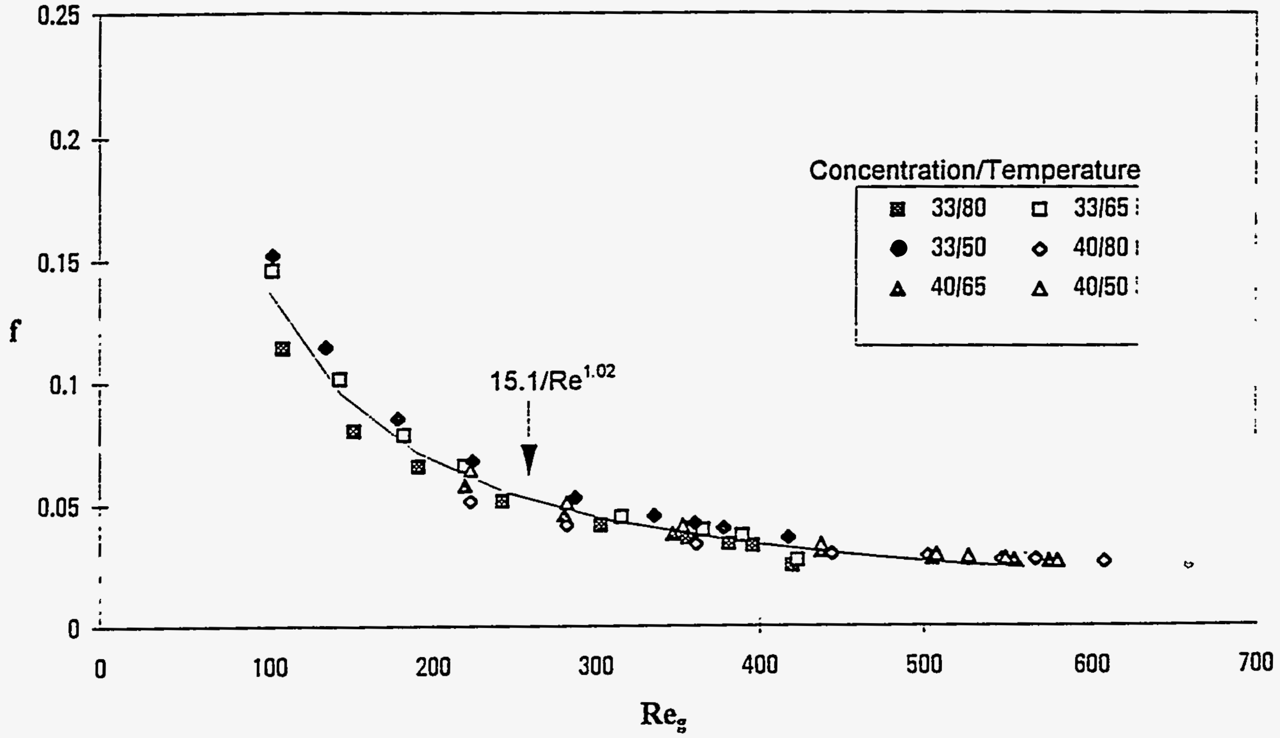

Fig. 8 The friction coefficient as a function of the general Reynolds number for the high solids concentration slurry.